Highlights

Integrated Basin Management Using System Dynamics: A Multi-Sectoral Modeling Framework under Climate Change

Takuya Nakashima

- System archetypes for integrated flood risk management are identified.
- A system dynamics model simulates green–gray strategies and their interactions.
- Policy mixes are evaluated through a virtual case across multiple RCP scenarios.

Integrated Basin Management Using System Dynamics: A Multi-Sectoral Modeling Framework under Climate Change

Takuya Nakashima[a,*]

[a] *Graduate School of Frontier Sciences, The University of Tokyo, Japan*

Abstract

This paper reframes basin-wide flood management as a coupled socio-ecological-infrastructure system and foregrounds structure over precision. We identify recurring system archetypes by mapping causal loops across green–gray measures, exposure dynamics, and governance incentives. Using reference modes and lightweight dynamic prototypes, we demonstrate how well-intended strategies can drift into decision traps and path dependence. We then derive leverage points and design propositions for portfolio planning (e.g., sequencing green and gray, guarding against safe-development paradox, protecting ecological base under fiscal stress). Validation is framed as future work via pattern-oriented and place-based assessment with stakeholders. We propose a conceptual, archetype-informed decision support that makes cross-sector feedback explicit and testable, providing a transparent bridge to subsequent quantitative and spatially resolved modeling.

Keywords: Climate Change, Adaptation, Systems Analysis, Integrated Flood Management, System Dynamics.

1. Introduction

Under climate change, the scale and frequency of heavy rainfall events are expected to increase, heightening the risk of water-related disasters. In Japan, this is further compounded by societal trends such as population aging and the concentration of people and assets due to compact city planning. Thus, beyond increasing hazards, greater attention must also be paid to the rise in exposure and vulnerability.

River basin disaster risk reduction (referred to as "basin-wide flood management" in this paper) aims to reduce these escalating risks through comprehensive interventions across catchment areas, river zones, and floodplains (Japan, 2024). This involves not only structural measures such as river improvement and dam construction, but also strategies to reduce exposure (e.g., relocation to lower-risk areas), early warning systems, land-use regulation, and measures for mitigating damage and facilitating early recovery. In addition, basin-wide management aligns well with nature-positive approaches like green infrastructure (e.g., wetlands, retention ponds), and achieving a balanced integration of green and grey infrastructure is critical to ensuring long-term sustainability and resilience (Kabisch et al., 2016).

Therefore, basin-wide flood risk management must consider not only hydrological impacts, but also ecological consequences, effects on agriculture due to the implementation of measures such as paddy field dams, and implications for urban development stemming from residential relocations. Moreover, since large river basins span multiple administrative regions, cross-regional and cross-sectoral impacts must be incorporated into planning, requiring consensus-building among a wide range of stakeholders.

Such multi-objective decision-making processes involving numerous stakeholders are inherently complex. While tools such as the "Climate Impact Chain" developed by GIZ exist to support qualitative understanding of climate-related interactions, these tools do not capture dynamic system behaviors (Zebisch et al., 2022). Therefore, dynamic simulation tools are necessary to evaluate future flood risks and adaptation strategies under changing climate conditions. However, the development and implementation of high-resolution, physically based models can be costly and time-consuming, making it difficult to assess combinations of diverse countermeasures (Brunner et al., 2021).

To address this, we aim to develop a general-purpose simulation model using system dynamics that can capture the interactions and effectiveness of basin-wide flood management strategies across upstream and downstream

*Corresponding author

Email address: nakashima@edu.k.u-tokyo.ac.jp (Takuya Nakashima)

regions. By simulating multiple policy combinations and analyzing decision patterns in a hypothetical urban setting, this study seeks to establish a general framework for evaluating and discussing basin-wide flood risk management.

Chapter 2 outlines the background on climate change and basin-wide flood risk management and discusses the need for decision support. Chapter 3 introduces system dynamics, presents archetype analysis using causal loop diagrams, and explains the model structure. Chapter 4 describes the case study of a virtual municipality and presents the simulation results. Chapter 5 discusses appropriate decision-making patterns based on the results, and Chapter 6 concludes the study.

2. Background

2.1. Climate Change and Basin-Wide Flood Management

Climate change has led to increasing concern over the intensification and frequency of extreme weather events, including heavy rainfall and flooding. In Japan, the extensive flooding that occurred in 2019 prompted the government to launch the concept of "River Basin Disaster Resilience and Sustainability by All (RBDRSA)" in 2020 (Japan, 2024). This initiative calls for holistic management of entire river basins—including headwater forests and agricultural areas in the upstream region, and urban zones downstream—beyond the conventional flood control measures limited to river channels and adjacent lands.

RBDRSA is based on three fundamental pillars: flood prevention, exposure reduction, and disaster resilience. Specific measures include:

1. Strengthening physical infrastructure such as levees and drainage systems,
2. Restricting development and promoting residential relocation from high-risk areas, and
3. Enhancing natural water retention capacity through afforestation, paddy field dams, and similar nature-based approaches.

While RBDRSA holds promise as an adaptation strategy that extends beyond flood prevention to address broader climate-related risks, several challenges remain. Among them is the need to incorporate green infrastructure—which involves greater uncertainty in effectiveness—into existing models traditionally based on grey infrastructure (Kabisch et al., 2016). Additionally, strong institutional coordination across administrative sectors and regions is essential.

2.2. Lack of Decision Support Tools

Effective adaptation requires collaboration among diverse stakeholders, each with their own values, priorities, and constraints. To facilitate such coordination, it is essential to understand the synergies and trade-offs between different policy options. However, many existing decision-support tools remain largely theoretical and are limited in their capacity to support practical, dynamic, and multi-objective decision-making.

As emphasized in the Sixth Assessment Report of the Intergovernmental Panel on Climate Change (IPCC AR6), adaptation planning still lacks practical tools that can effectively model feedback loops, stakeholder behavior, and long-term policy interactions Intergovernmental Panel On Climate Change (IPCC) (2023). This underscores the need for dynamic modeling frameworks that can support integrated planning and participatory decision-making under uncertainty.

2.3. Research Purpose

This study develops a comprehensive, simulation-based evaluation framework using system dynamics (SD) to analyze interactions between policies, infrastructure, ecosystems, and human behavior over time. We aim to provide a decision-support tool for municipalities to explore the effectiveness and unintended consequences of different river basin adaptation strategies.

3. Method

3.1. System Dynamics

System dynamics is a modeling approach designed to analyze problems characterized by complex dynamics and uncertainty (Sterman, 2000). It has been successfully applied in the context of flood risk management (Ahmad and Simonovic, 2000). In addition to its capacity for numerical simulation, system dynamics employs stock-and-flow diagrams to visualize the relationships and causal linkages among events and interventions. This dual capability

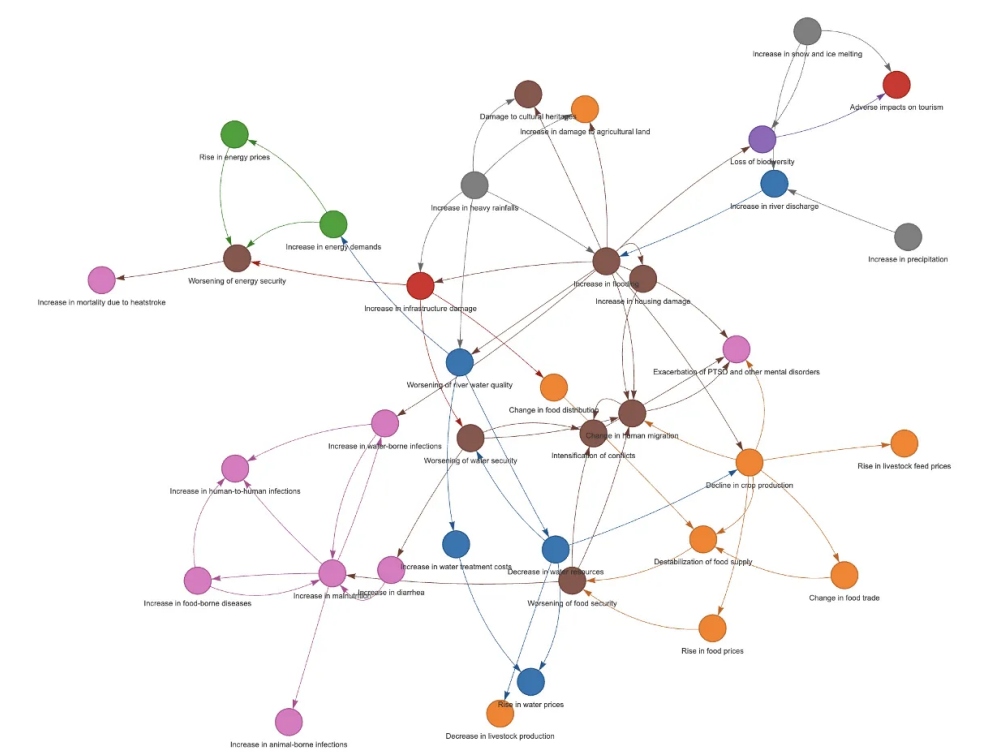

Fig. 1: Impact Network by Yokohata et al. (2019)

facilitates discussions on the validity and scalability of the model structure, making system dynamics an appropriate choice for our study (Awah et al., 2024).

Compared to process-based models that require detailed terrain and hydrological data, this approach significantly reduces the development time. Moreover, it enables an evaluation of broad societal and economic impacts as well as the cascading effects of various policy measures, thereby potentially providing valuable insights for local governments planning basin-wide flood management and climate change adaptation strategies.

3.2. System of Interest

The model focuses on a river basin system that is, directly or indirectly, affected by an increase in flooding, as illustrated in the schematic extracted from Yokohata et al. (2019):

3.3. Causal Loop Diagrams and Archetype Analysis

To comprehensively evaluate policy interventions related to basin-wide flood management, a Causal Loop Diagram (CLD) was developed (see Figure 2). The analysis identified several typical system archetypes, which reflect structural challenges often observed in real-world flood management initiatives. Table 1 summarizes the observed archetypes. These archetypes not only help elucidate the effects and limitations of individual measures but also provide critical insights into the interactions and underlying systemic issues arising from the combination of various policies. Consequently, they underscore the necessity of multi-layered and integrated strategies for effective flood management.

Importantly, these system archetypes align closely with well-known socio-hydrological phenomena, as identified by de Baldassarre et al. (2019). For example, the “Fixes that Fail” archetype corresponds to the “supply-demand cycle”, in which increasing flood protection or water supply (e.g., through dam or levee construction) initially alleviates problems but ultimately leads to increased development and exposure, thereby worsening long-term risk (Gohari et al., 2013). Conversely, the “Shifting the Burden” archetype mirrors the “safe-development paradox”, where reliance on symptomatic responses such as emergency evacuation and recovery reduces the incentive to address underlying vulnerabilities, such as land use change or upstream deforestation (de Baldassarre et al., 2019). Similarly, the “Success to the Successful” archetype is related to the “aggregation effect”, where disproportionate resource allocation to already resilient areas reinforces inequality, leaving vulnerable regions with inadequate protection and increasing long-term risk.

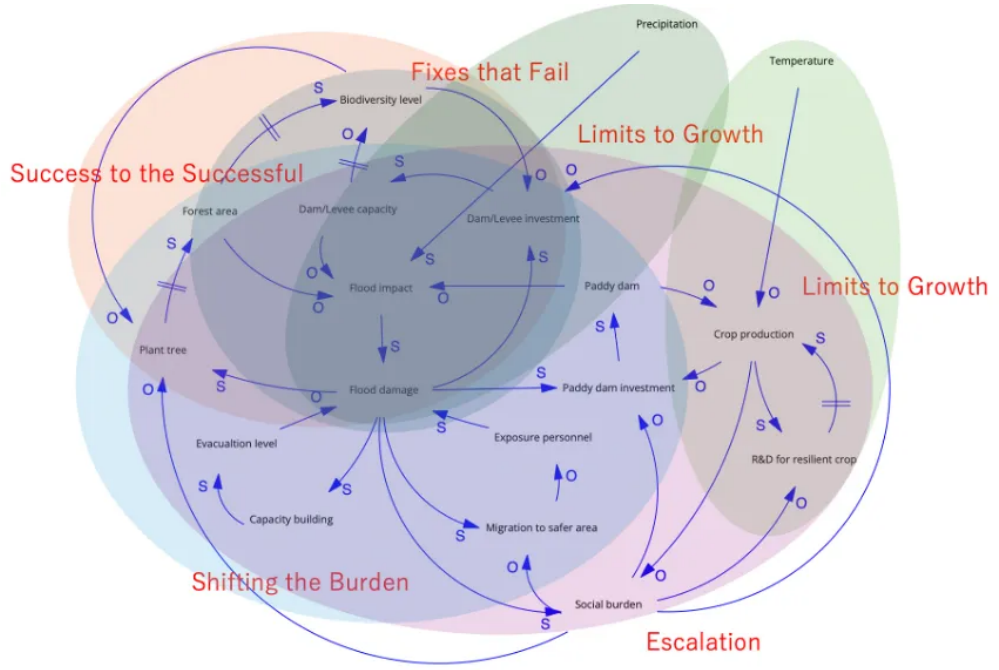

Fig. 2: Causal Loop Diagram for Basin-Wide Flood Management

Table 1: System Archetypes in Basin-Wide Flood Management

Archetype	**Description**	**Simulation Structure**
Fixes that Fail	Short-term fixes worsen the problem in the long run.	Temporary flood mitigation via levee construction → ecosystem degradation.
Shifting the Burden	Reliance on symptomatic solutions, which delays addressing root causes.	Disaster response through relocation and public drills → postponement of forest conservation and dam construction.
Limits to Growth	Early success is halted by constraints.	The effectiveness of dam construction and R&D reaches a plateau under rising temperatures and extreme precipitation.
Success to the Successful	Resources are increasingly allocated to winners, widening disparities.	Concentration of infrastructure investments → delayed ecosystem degradation that weakens incentives for afforestation.
Escalation	Competitive responses lead to a negative spiral.	Increased social burdens from flooding hinder further investments (negative feedback loop).

3.4. Construction of the System Dynamics Model

In our model, interactions among multiple domains—including climate variability, residential behavior, and public investment—are integrated to quantitatively evaluate the effects of future climate change adaptation policies. Annually, the model updates the state of both social and natural environments and simulates their responses to policy interventions (decision variables).

It is important to note that the model assumes a closed system. For example, spillover effects of agricultural R&D improvements or water inflows from outside the modeled area are not considered.

Further details are provided in the Appendix. Initially, a stock-flow diagram was developed using Vensim; however, considering the flexibility of the interface, the model has been implemented using Python.

4. Case Study

4.1. Model Setup

In this case study, we consider a hypothetical river basin. The total area is assumed to be 100 km^2 (10,000 ha), traversed by approximately 20 km of river. The land use is distributed as follows: 70% forest, 10% paddy fields, and 5% residential areas. Residential zones are assumed to be located near the river, making them vulnerable to flooding.

The population is set at 34,000 people (based on Japan's national average of 340 persons/km^2), with approximately 15,000 households (assuming an average household size of 2.23).

Regarding the hydrological balance: 35% of precipitation is assumed to evapotranspire, while 55% becomes river runoff (Oki et al., 2005). Annual water usage is divided into 110 mm for domestic use (including industrial water), 220 mm for industrial use, and 300 mm for agriculture.

A dynamic simulation model is constructed with an annual time step to simulate policy decisions over a 75-year period from 2026 to 2100. External climate uncertainties are represented using a range of Representative Concentration Pathways (RCPs), from 1.9 to 8.5.

4.2. Decision Variables

The model includes the following policy decision variables (intervention elements):

- Afforestation and forest conservation (area in ha) [Upstream]
- Levee and dam construction (investment amount) [Upstream]
- Residential relocation (number of households) [Downstream]
- Disaster education and awareness programs (investment amount) [Downstream]

Policy decisions are assumed to be consistent across generations and are updated every 25 years. For each decision variable, one of the available intervention strategies is selected per period.

4.3. Output Indicators

The model generates the following annual indicators to evaluate the impact of various policy scenarios:

- Estimated flood damage cost
- Ecosystem health index
- Resident burden (public expenditure + damage cost per capita)

These outputs are tracked over time and analyzed across different scenarios.

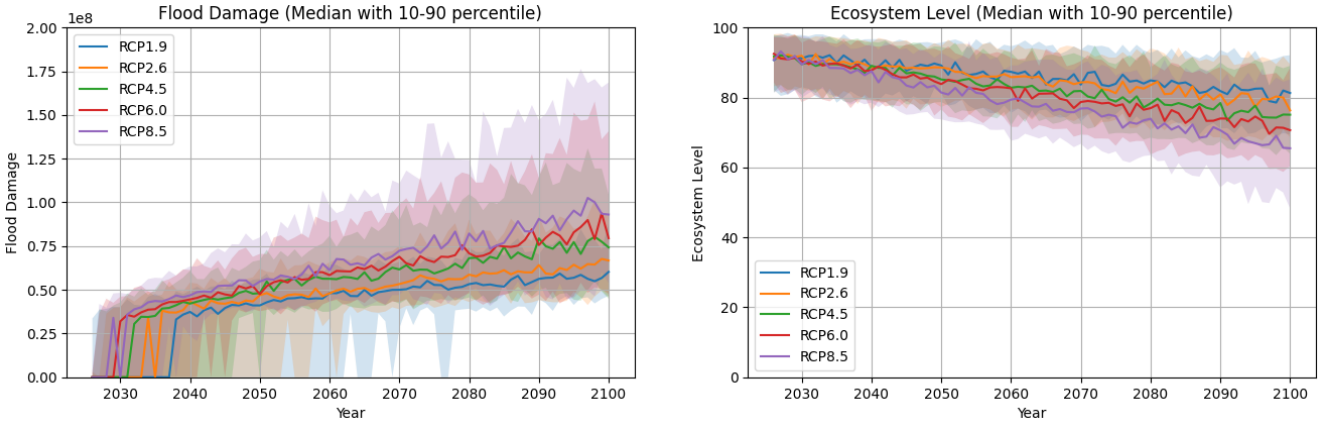

Fig. 3: Flood damage and ecosystem level forecasting results without any additional policies.

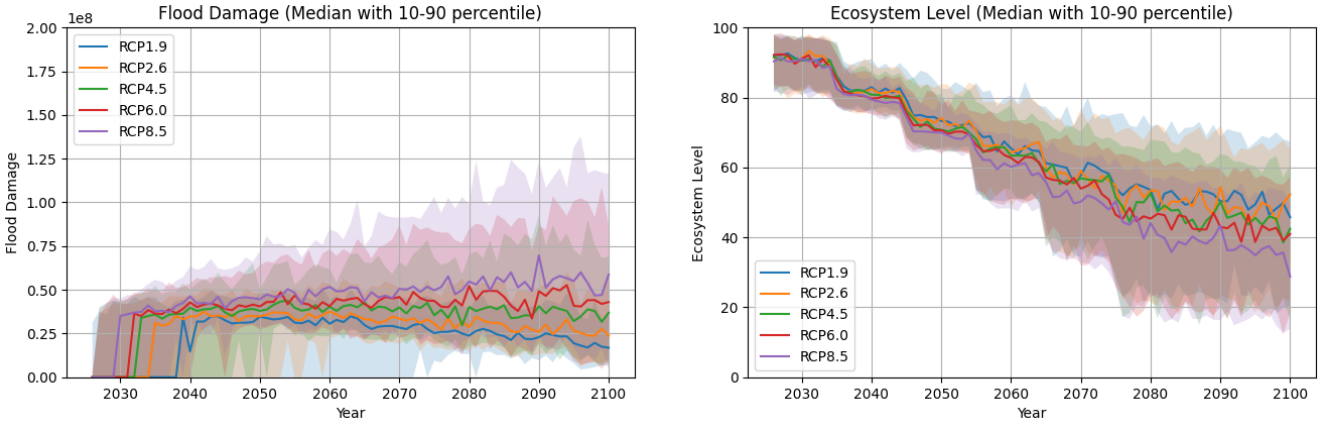

Fig. 4: Flood damage and ecosystem level forecasting results focusing only on Levee investment.

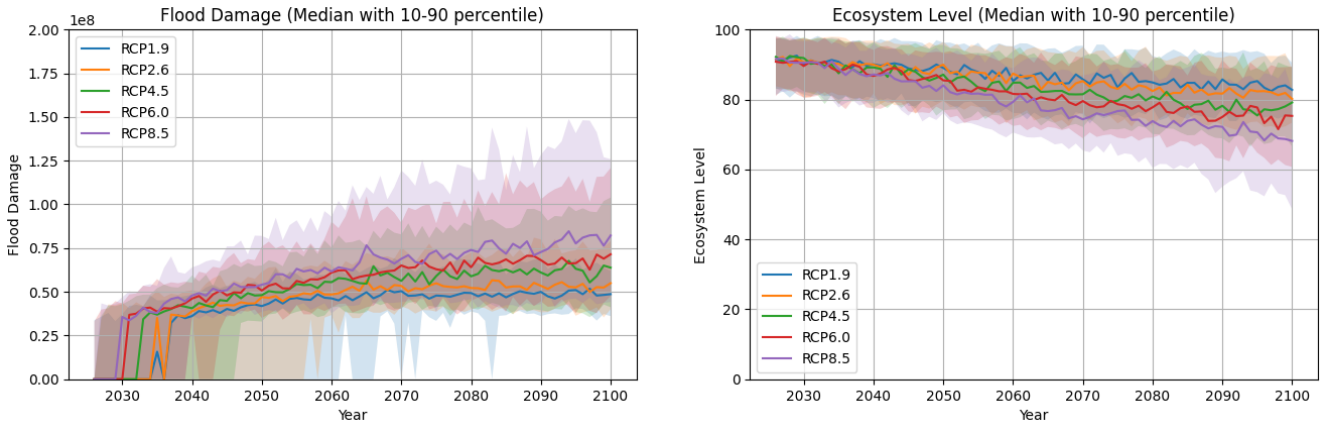

Fig. 5: Flood damage and ecosystem level forecasting results focusing only on Forestation.

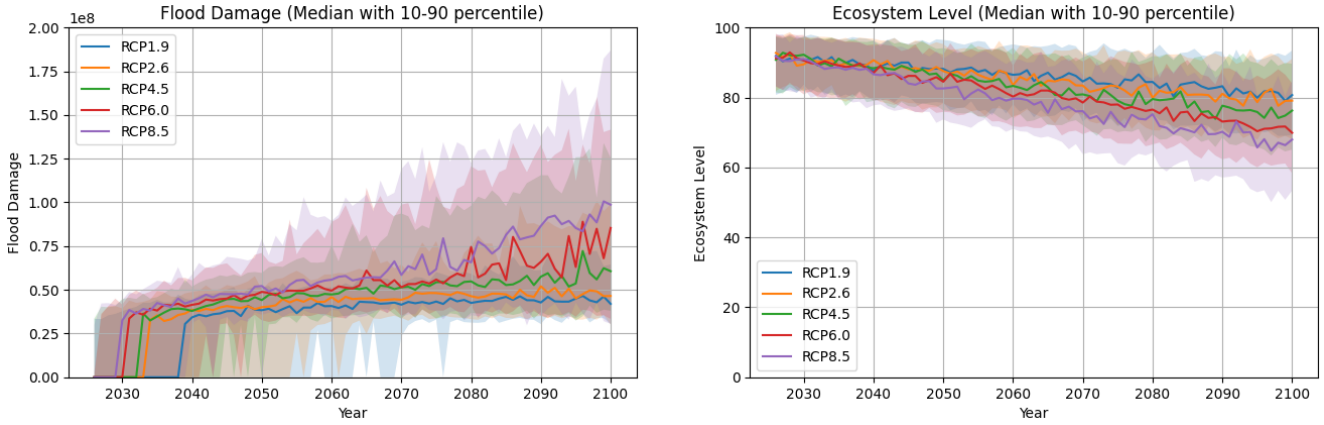

Fig. 6: Flood damage and ecosystem level forecasting results focusing only on migration.

4.4. Simulation Results

4.4.1. Baseline Case

We first present the evaluation results for the No Additional Measures scenario in Fig. 3. As expected, the projected damages increase progressively with higher RCP values. Notably, this increase is not linear; rather, under RCP8.5, the damages escalate significantly in the latter half of the simulation period.

Fig. 4 also shows the scenario focusing solely on investments in gray infrastructure, such as levee and dam construction. While this approach substantially reduces flood risks, as anticipated, it also results in extremely high financial burdens on residents—raising concerns about feasibility. Furthermore, the degradation of ecosystem health under this scenario is considerable.

Fig. 5 displays the afforestation-focused scenario. Although tree planting requires a longer time horizon to deliver visible effects, its gradual impact aligns well with the progressively intensifying effects of climate change. However, the contribution of afforestation alone to improving ecosystem conditions is limited. Its full effectiveness appears to be realized only when combined with gray infrastructure.

Next, the scenario centered on residential relocation is shown in Fig. 6. This approach proves effective, particularly under low RCP conditions, but fails to maintain effectiveness under more severe climate scenarios.

The disaster preparedness-focused scenario is also illustrated in Fig. 7. While it offers some initial benefits, its effectiveness plateaus and eventually diminishes once the climate impacts exceed a certain threshold.

These findings collectively suggest that no single policy measure is sufficient on its own. Each has its trade-offs and limitations. Therefore, it is desirable to explore and evaluate policy mixes that combine multiple measures to achieve more robust and sustainable adaptation outcomes.

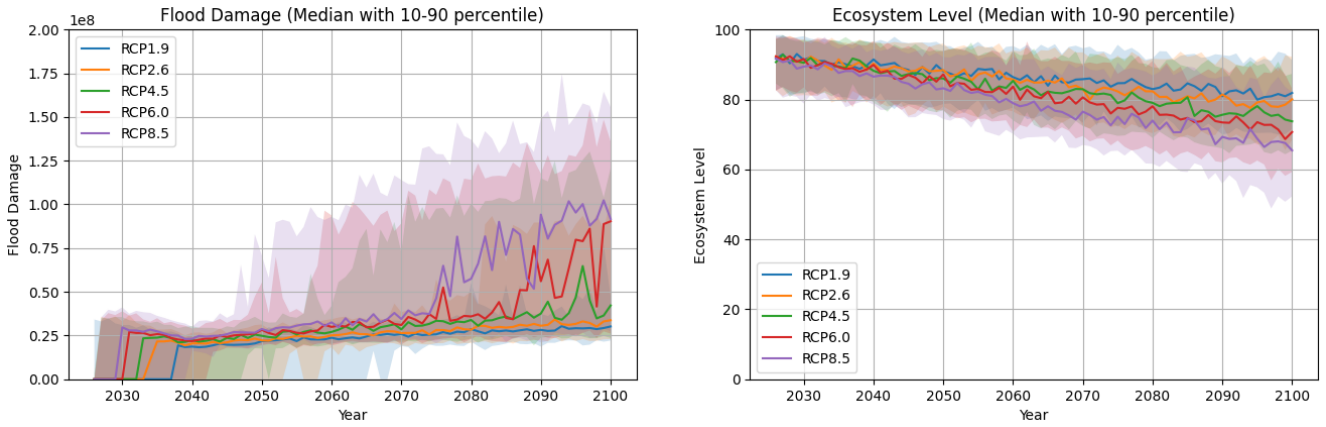

Fig. 7: Flood damage and ecosystem level forecasting results focusing only on capacity building.

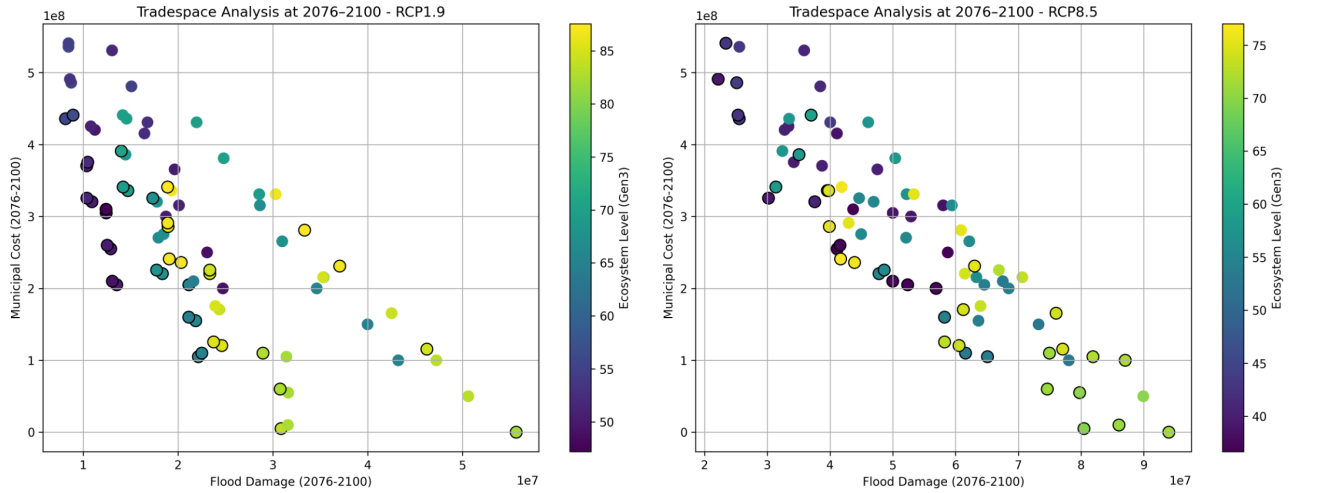

Fig. 8: Tradespace analysis of combinations of policy decisions with different RCP scenarios.

4.4.2. Multiple Case

As a first step, we examined the optimal combinations of policy decisions while keeping the decision pattern fixed across all time periods. Based on Fig. 8, we found that the combinations of measures forming the Pareto front differ significantly between RCP1.9 and RCP8.5 scenarios. Overall, scenarios that rely heavily on levee reinforcement tend to be part of the Pareto front under RCP1.9. However, under the more severe RCP8.5 scenario, the relative advantage of afforestation-oriented strategies becomes more prominent, indicating a shift in the effectiveness of adaptation approaches as climate risks intensify.

5. Discussion

5.1. Scenario Analysis and Implications

The results of our scenario simulations reveal that no single policy intervention is sufficient to address the multifaceted challenges of basin-wide flood risk under climate change. Instead, a combination of measures—adaptively selected over time and across regions—is necessary to achieve balanced outcomes in terms of flood risk reduction, ecosystem preservation, agricultural productivity, and resident welfare.

Several scenario clusters emerged as viable policy pathways, each with its own trade-offs. For example, early investment in afforestation proves beneficial in the long term, especially when used to buffer future uncertainty. Conversely, overreliance on grey infrastructure can lead to excessive financial burdens and ecological degradation. These findings highlight the importance of long-term, multi-layered strategies that integrate both green and grey infrastructure components.

5.2. Archetype Dynamics Observed in Simulation Results

The simulation results reflect several classic system archetypes:

- **Fixes that Fail**: In the levee-only scenario (Fig. 4), short-term reductions in flood damage led to long-term ecosystem degradation and increased resident burden, validating the classic pattern of unintended consequences.
- **Shifting the Burden**: The relocation-focused strategy (Fig. 6) reveals initial reductions in risk, but failure to invest in upstream ecological functions leads to vulnerability later in the century under RCP8.5.
- **Limits to Growth**: The afforestation-only strategy (Fig. 5) demonstrates diminishing returns, especially when forest expansion is constrained and damage outpaces ecosystem benefits.
- **Success to the Successful**: In the policy-mix exploration (Fig. 8), strategies that initially favored infrastructure tend to reinforce investment in gray measures, sidelining nature-based solutions in later decades.
- **Escalation**: Under scenarios with delayed policy response, the simulation shows increasing damage and rising public cost, leaving fewer resources for proactive investment—illustrating a negative feedback spiral.

5.3. Limitations and Future Work

This study has several limitations that warrant further investigation:

- **Limited scope of flood risk measures:** Key interventions such as dam development and land-use zoning policies were either simplified or excluded in this model. Future models should incorporate a wider range of countermeasures.
- **Lack of spatial resolution:** The model does not account for spatial heterogeneity, which limits its ability to evaluate biodiversity impacts or local land-use conflicts.
- **Model validation:** While the model reproduces several "stylized facts" consistent with real-world trends, formal validation has not been conducted. Future research should involve empirical calibration and case-specific data collection.
- **Parameter generality:** The model is based on generalized parameters. Tailoring the model to specific regions will improve its relevance and accuracy.
- **Decision dynamics:** Although system archetypes were identified, the model does not yet sufficiently capture the temporal evolution of stakeholder decisions in response to changing conditions. Incorporating dynamic decision rules remains an important future task.

Ultimately, to fully assess the impacts of basin-wide flood management, future models should be expanded to simulate physical water flows and spatial interactions under different climate and land-use scenarios.

6. Conclusion

This study developed a general-purpose simulation model using system dynamics to assess the interactions and effects of basin-wide flood risk management policies across upstream and downstream areas of a river system. By analyzing the combinations of various policy interventions, we explored decision-making patterns that could lead to sustainable outcomes in a hypothetical urban setting.

Despite its limitations, the model successfully provides a conceptual framework for understanding the complex trade-offs involved in integrated flood risk management under climate change. Our findings underscore the importance of combining structural and non-structural measures, integrating green and grey infrastructure, and coordinating actions across stakeholders and timeframes.

Through archetype analysis, this study further revealed that well-intentioned policies may fall into structural traps. In particular, strategies focused solely on reducing exposure (e.g., relocation) or mitigating damage (e.g., infrastructure investment) are vulnerable to the "Shifting the Burden" archetype, where root causes such as ecosystem degradation remain unaddressed. Similarly, we observed a "Limits to Growth" dynamic in afforestation strategies, where initial benefits plateau under increasing climate stress. Moreover, "Success to the Successful" dynamics showed how early investment patterns can bias future decisions, reinforcing infrastructure-centric paths at the expense of long-term ecological resilience.

These findings demonstrate that integrated and adaptive planning is necessary not only to reduce risks, but also to avoid path dependencies and unintended consequences. Recognizing and addressing these systemic feedbacks is essential for developing robust, equitable, and forward-looking adaptation strategies.

This general framework may serve as a foundation for future discussions and developments in climate adaptation planning, especially in contexts where interdisciplinary and intergenerational decision-making is essential.

Acknowledgment

The authors would like to express their sincere gratitude to the SECOM Science and Technology Foundation for the financial support of this research.

Appendix: Details of the Constructed Model

1. Climate Parameter Settings

Climate parameters are set based on RCP scenarios. While actual regional applications should ideally use projections from climate models or integrated datasets, here, future trends are modeled using deterministic trends and random perturbations.

Mean Annual Temperature T_0 is initialized at 15.5°C (based on the average of AMEDAS stations in Japan), with a linear increase (α_T) depending on the RCP scenario. Annual variability σ_T is modeled as a Gaussian distribution with a fixed standard deviation of 0.5°C:

$$\text{Temp}_t = T_0 + \alpha_T(t - t_0) + \mathcal{N}(0, \sigma_T)$$

Mean Annual Precipitation P_0 is set at 1,700 mm, with a fixed average (α_P is set as zero) and RCP-dependent variability $\sigma_{P,t}$:

$$\text{Precip}_t = \max\left(0, P_0 + \alpha_P(t - t_0) + \mathcal{N}(0, \sigma_{P,t})\right)$$

where $\sigma_{P,t} = \sigma_{P,0} + \alpha_{\sigma_P}(t - t_0)$ increases under higher RCP scenarios.

Extreme Precipitation Events are modeled with a two-step approach:

- Frequency per Year: Poisson distribution

$$\lambda_t = \max(0, \lambda_0 + \alpha_\lambda(t - t_0))$$

$$N_{\text{extreme}} \sim \text{Poisson}(\lambda_t)$$

- Intensity per Event: Gumbel distribution (extreme value)

$$\mu_t = \max(\mu_0 + \alpha_\mu(t - t_0), 0)$$

$$\beta_t = \max(\beta_0 + \alpha_\mu(t - t_0), 0)$$

$$\text{RainEvent}_i \sim \text{Gumbel}(\mu_t, \beta_t), \quad i = 1, \ldots, N_{\text{extreme}}$$

Here, λ_0 is set at 0.1 times per year. μ_0 and β_0 are set at 180 and 20, respectively. α_λ, and α_μ are set based on RCP scenarios.

Table .2: Parameter trends under each RCP scenario

Parameter	RCP 1.9	RCP 2.6	RCP 4.5	RCP 6.0	RCP 8.5
α_T	0.020	0.025	0.035	0.045	0.060
α_{σ_P}	0.000	0.000	1.500	2.000	3.000
α_λ	0.050	0.070	0.100	0.130	0.170
α_μ	0.200	0.400	0.800	1.100	1.500

2. Socio-environmental Scenario

Water demand from residents is modeled based on annual population growth and stochastic variability:

$$\text{Demand}_t = \text{Demand}_{t-1} \cdot (1 + \gamma + \mathcal{N}(0, \sigma_\gamma))$$

Annual growth is assumed constant (γ is set at zero), and inter-annual variation σ_γ is set at 1%.

3. Forest Module

Forest area changes based on afforestation and natural degradation. The cost of afforestation is 2,410,000 [Yen/ha] (Kochi Prefecture, Department of Agriculture, Forestry and Fisheries, Land Improvement Division, 2015), with 1,000 cedar trees planted per hectare (Okayama Prefecture, 2019). Soil water retention is assumed to activate after Y_g years. Here we set Y_g as 30. Loss ratio r_d is set at 0.01

$$\text{MaturedTrees}_t = \text{Planting}_{t-Y_g}$$

$$\text{Loss} = A_{f,t-1} \cdot r_d$$

$$A_{f,t} = \max(A_{f,t-1} + \text{MaturedTrees}_t - \text{Loss}, 0)$$

The flood reduction effect is modeled as the relative increase in forest area compared to its initial proportion, scaled by a sensitivity coefficient α_{flood}:

$$\text{FloodReduction}_t = \alpha_{\text{flood}} \cdot \left(\frac{A_{f,t} - A_{\text{total}} \cdot r_{f,0}}{A_{\text{total}}} \right) \tag{.1}$$

where $A_{f,t}$ is the forest area at time t, A_{total} is the total area, and $r_{f,0}$ α_{flood} was set in the range of 0.4–2.8 based on the empirical findings of Bradshaw et al. (2007), and varied randomly for each simulation trial.

The water retention boost from forests is proportional to the current forest coverage, with a sensitivity coefficient α_{water}:

$$\text{WaterRetention}_t = \alpha_{\text{water}} \cdot \frac{A_{f,t}}{A_{\text{total}}} \tag{.2}$$

α_{water} was set in the range of 2.0–4.0 based on Bosch and Hewlett (1982), and varied randomly for each simulation trial.

4. Water Resource Module

Water availability is updated dynamically considering precipitation, evapotranspiration, demand, and forest effects. Maximum water level $W_{\max}$ is capped at 3000 mm. If water drops below 800 mm, ecosystem damage occurs.These values should be calibrated to match the specific water storage capacity, land cover, and hydrological conditions of the target region. The runoff coefficient θ was set to 0.55. Evapotranspiration is set to increase 5% per +1°C rise based on Clausius–Clapeyron equation:

$$ET_t = ET_0 \cdot (1 + 0.05 \cdot (\text{Temp}_t - T_0))$$

$$W_t = \min\left(\max\left(W_{t-1} + \text{Precip}_t - ET_t - \text{Demand}_t - \theta \cdot \text{Precip}_t + \text{WaterRetention}_t \cdot \text{Precip}_t, 0\right), W_{\max}\right)$$

5. Agriculture Module

Let the following variables be defined:

- T_t: Annual average temperature in year t
- T_{tol}: Crop high-temperature tolerance level
- $L_T(T_t, T_{\text{tol}})$: Yield loss due to temperature stress
- $A_{\text{dam},t}$: Area of paddy fields converted to paddy dams at year t
- A_{paddy}: Total area of paddy fields

- ρ_{dam}: Yield reduction coefficient due to paddy dam use (e.g., 0.01)
- W_t: Available agricultural water in year t
- W_{need}: Water required to meet full agricultural demand
- $Y_{\max}$: Maximum attainable yield [ton/ha]
- I_t: Investment in paddy dam construction in year t
- C_{dam}: Cost per hectare to construct paddy dams (e.g., 1,500,000 yen/ha)

$$L_T = \text{estimate\_rice\_yield\_loss}(T_t, T_{\text{tol}})$$

$$A_{\text{dam},t} = A_{\text{dam},t-1} + \frac{I_t}{C_{\text{dam}}}$$

$$L_{\text{dam},t} = \rho_{\text{dam}} \cdot \min\left(\frac{A_{\text{dam},t}}{A_{\text{paddy}}},\ 1\right)$$

$$W_{\text{factor},t} = \min\left(\frac{W_t}{W_{\text{need}}},\ 1\right)$$

$$Y_t = \max\left[Y_{\max} \cdot (1 - L_T) \cdot W_{\text{factor},t} \cdot (1 - L_{\text{dam},t}),\ 0\right]$$

Agricultural yield reduction due to heat stress is modeled during the ripening phase.

The ripening-phase nighttime temperature is assumed to be $\text{Temp}_t + 6$°C based on typical seasonal elevation over the annual average. Based on Su et al. (2023), yield is maximized in the range of 20–22°C. Yield declines at a rate of 4% per °C between 22°C and a turn-point (30°C by default), and at 10% per °C beyond that. The thresholds are increased by heat tolerance level T_{tol}, which is endogenously determined through R&D.

$$T_{\text{ripening}} = \text{Temp}_t + 6$$

$$T_{\text{opt}} = 22 + T_{\text{tol}}, \quad T_{\text{turn}} = 30 + T_{\text{tol}}, \quad T_{\min} = 20$$

$$L_T = \begin{cases} 0 & \text{if } T_{\text{ripening}} \leq T_{\min} \\ (T_{\min} - T_{\text{ripening}}) \cdot 0.10 & \text{if } T_{\text{ripening}} < T_{\text{opt}} \\ (T_{\text{ripening}} - T_{\text{opt}}) \cdot 0.04 & \text{if } T_{\text{opt}} \leq T_{\text{ripening}} \leq T_{\text{turn}} \\ (T_{\text{turn}} - T_{\text{opt}}) \cdot 0.04 + (T_{\text{ripening}} - T_{\text{turn}}) \cdot 0.10 & \text{if } T_{\text{ripening}} > T_{\text{turn}} \end{cases}$$

where $T_{\text{R\&D}} = 5{,}000{,}000$ [Yen] and $Y_{\text{R\&D}} = 5$ [years]. If the threshold is met or exceeded, the crop heat tolerance level is increased by a fixed increment $\Delta T_{\text{tol}} = 0.2$°C, and the investment counter is reset.

To enable flood mitigation using rice paddies (so-called "paddy dams"), ordinary fields must be converted into controllable storage-enabled paddies. This conversion requires an investment cost of 1,500,000 [Yen/ha]. Once converted, these paddies serve as retention areas during heavy rainfall events. However, such use imposes additional management burdens and constraints on cultivation. Therefore, we assume a 1% yield reduction for the area converted into paddy dams. This penalty is linearly applied to the proportion of total agricultural land under paddy-dam usage.

6. Residential Module

Relocation from high-risk housing reduces flood vulnerability. Each relocation costs 975,000 Yen per household (Ministry of Land, Infrastructure, Transport and Tourism, 2016).

$$H_r = \max(H_{r,t-1} - M_t, 0) \quad H_s = H_{s,t-1} + M_t \quad R_t = \frac{H_s}{H_r + H_s}$$

7. Infrastructure Module

Levee and paddy-dam investment is modeled as a probabilistic threshold function. A 20 km levee project costs 4 billion Yen and withstands +20 mm rainfall. Initial

$$I_{\text{levee},t} = I_{\text{levee},t-1} + C_{\text{levee}}$$

$$\text{If } I_{\text{levee},t} \geq \mathcal{N}(T_L, 0.01 \cdot T_L): \quad L_t += \Delta L, \quad I_{\text{levee},t} = I_{\text{levee},t} - \mathcal{N}(\cdot)$$

Each year, the cumulative investment in levee construction $I_{\text{levee},t}$ increases by a fixed annual amount C_{levee}. When the accumulated investment exceeds a stochastic threshold drawn from a normal distribution centered at $T_L = 20$ (million yen) with a standard deviation of 1%, a new levee segment is added. The levee protection level L_t is incremented by $\Delta L = 20$ (mm), and the investment counter is partially reset by subtracting the realization from the distribution.

8. Flood Damage

Flood damage is modeled by considering the protective effects of paddy-dam areas and levee infrastructure, along with forest-based flood mitigation and resident preparedness.

Paddies are assumed to have a water retention capacity of 1,000 [m^3/ha] when used as paddy dams. Through investment, this proportion can be increased, and the total paddy-dam storage capacity is calculated as a function of the converted area. Although in practice, water control operations are essential to maximize effectiveness, this model simplifies the effect by treating paddies as static retention capacity during extreme rainfall events. The base mitigation effect from paddy-dam infrastructure is defined as:

$$\phi_{\text{paddy-flood}} = \rho_{\text{paddy-flood}} \cdot \frac{A_{\text{paddy}}}{A_{\text{paddy, total}}}$$

Where $\rho_{\text{paddy-flood}}$ is set as 10, which assumes that the paddy dam can store an additional 10 cm of heavy precipitation.

For each extreme rainfall event R_i, the overflow amount beyond protection capacity (levee level plus paddy-dam level) is used to compute the initial flood damage D_{flood}:

$$D_{\text{flood}} = \sum_{i=1}^{N} \max(R_i - L_t - \phi_{\text{paddy-flood}}, 0) \cdot (1 - \text{FloodReduction}_t) \cdot \rho_D$$

where ρ_D is set as 100,000 (yen/mm). Actual damage is then calculated based on adaptive capacity by residents and local training awareness.

$$\text{response\_factor}_i = \frac{1}{1 + \exp\left(-\beta(R_i - L_t - \phi_{\text{paddy-flood}} - \tau)\right)}$$

where β controls the slope (e.g., 0.1) and τ represents a stress threshold set as 400 mm. The residual flood damage after accounting for preparedness (R_t) and training level (C_t) is:

$$D_{\text{actual}} = D_{\text{flood}} \cdot (1 - R_t) \cdot (1 - C_t)$$

Finally, agricultural output is reduced proportionally to flood impact:

$$Y_t = Y_t - D_{\text{actual}} \cdot \rho_Y$$

where ρ_Y is set as 0.00001 (ton/ha/Yen). This formulation allows nonlinear degradation of protective behavior when flood severity surpasses critical thresholds, and integrates both structural and social countermeasures.

9. Ecosystem Evaluation

The ecosystem level at each simulation step is calculated as a weighted aggregation of three components: natural resource base, disturbance resistance, and human pressure, based on the framework proposed by Kristensen (2004). These components are normalized between 0 and 1 and then scaled to a 0–100 score.

Natural Resource Base reflects the extent of available forest area and water resources:

$$\text{EcologicalBase} = 0.5 \cdot \min\left(\frac{A_{f,t}}{A_{\text{total}}}, 1.0\right) + 0.5 \cdot \min\left(\frac{W_t}{W_{\text{threshold}}}, 1.0\right) \tag{.3}$$

where:

- $A_{f,t}$: forest area at year t,
- A_{total}: total simulation area,
- W_t: available water at year t,
- $W_{\text{threshold}}$: ecosystem water threshold.

Disturbance Resistance models the ecosystem's capacity to withstand climate-induced stress, particularly from temperature anomalies and extreme precipitation events. It is formulated as:

$$\text{Resistance}_t = \max\left(0,\ 1.0 - \beta_T \cdot |T_t - T_0| - \beta_P \cdot N_{\text{extreme},t}\right) \tag{.4}$$

where T_t is the mean annual temperature at year t, T_0 is the baseline reference temperature (e.g., 2000–2020 average), $N_{\text{extreme},t}$ is the number of extreme precipitation events in year t, β_T and β_P are sensitivity coefficients that represent the impact of temperature deviation and precipitation extremes, respectively.

Based on empirical ecological vulnerability assessments under climate variability (on Climate Change, 2022; Thuiller et al., 2005; Urban, 2015), we assume $\beta_T = 0.05$ and $\beta_P = 0.03$ as baseline values. These reflect moderate ecosystem sensitivity to physical climate stressors in temperate regions.

Human Pressure penalizes intensive human intervention in river systems, especially through extensive levee construction, which reduces ecosystem connectivity and resilience:

$$\text{HumanPressure}_t = 1.0 - \min(\beta_L \cdot L_t,\ 1.0) \tag{.5}$$

where L_t denotes the levee protection level at year t (normalized). β_L is a scaling coefficient, set to $\beta_L = 0.01$ in accordance with studies on ecological disruption due to hard infrastructure.

The final ecosystem level is computed as a weighted sum of the three components:

$$\text{EcosystemLevel}_t = 100 \cdot (w_1 \cdot \text{EcologicalBase} + w_2 \cdot \text{Resistance} + w_3 \cdot \text{HumanPressure}) \tag{.6}$$

where the weights (w_1, w_2, w_3) are sampled from a Dirichlet distribution to reflect uncertain or variable relative importance.

10. Public Awareness Module

Disaster preparedness awareness degrades over time, but can be improved via investment:

$$C_t = C_{t-1} \cdot (1 - \delta_C) + C_{\text{train}} \cdot \rho_C \quad C_t = \min(C_t, C_{\max})$$

where δ_C, ρ_C, and $C_{\max}$ are set as 0.05, 0.01, and 0.99, respectively.

11. Cost Evaluation Module

Total public cost is calculated from infrastructure, disaster recovery, and relocation expenses:

$$C_{\text{tree}} = P_{\text{tree}} \cdot N_{\text{tree}}, \quad C_{\text{migrate}} = P_{\text{mig}} \cdot N_{\text{mig}}$$

$$C_{\text{total}} = C_{\text{levee}} + C_{\text{R\&D}} + C_{\text{paddy}} + C_{\text{train}} + C_{\text{tree}} + C_{\text{migrate}} + C_{\text{trans}}$$

$$B_t = C_{\text{total}} + D_{\text{actual}} \cdot \rho_{\text{recover}}$$

where ρ_{recover} is set as 0.1.

References

Ahmad, S., Simonovic, S.P., 2000. System dynamics modeling of reservoir operations for flood management. Journal of Computing in Civil Engineering 14, 190–198. doi:10.1061/(ASCE)0887-3801(2000)14:3(190).

Awah, L.S., Belle, J.A., Nyam, Y.S., Orimoloye, I.R., 2024. A systematic analysis of systems approach and flood risk management research: Trends, gaps, and opportunities. International Journal of Disaster Risk Science 15, 45–57. URL: https://link.springer.com/article/10.1007/s13753-024-00522-y, doi:10.1007/s13753-024-00522-y. open Access.

de Baldassarre, G., Sivapalan, M., Rusca, M., Cudennec, C., Garcia, M., Kreibich, H., Konar, M., Mondino, E., Mård, J., Pande, S., Sanderson, M.R., Tian, F., Viglione, A., Ward, P.J., Van Loon, A.F., 2019. Sociohydrology: Scientific challenges in addressing the sustainable development goals. Water Resources Research 55, 6327–6355. doi:10.1029/2018WR023901.

Bosch, J.M., Hewlett, J.D., 1982. A review of catchment experiments to determine the effect of vegetation changes on water yield and evapotranspiration. Journal of Hydrology 55, 3–23. URL: https://doi.org/10.1016/0022-1694(82)90117-2, doi:10.1016/0022-1694(82)90117-2.

Bradshaw, C.J.A., Sodhi, N.S., Peh, K.S.H., Brook, B.W., 2007. Global evidence that deforestation amplifies flood risk and severity in the developing world. Global Change Biology 13, 2379–2395. URL: https://doi.org/10.1111/j.1365-2486.2007.01446.x, doi:10.1111/j.1365-2486.2007.01446.x.

Brunner, M.I., Clark, M., Slater, L., Tallaksen, L., 2021. Challenges in modeling and predicting floods and droughts: A review. Wiley Interdisciplinary Reviews: Water 8, e1520. URL: https://doi.org/10.1002/wat2.1520, doi:10.1002/wat2.1520.

on Climate Change, I.P., 2022. Climate change 2022: Impacts, adaptation and vulnerability. Sixth Assessment Report .

Gohari, A., Eslamian, S., Mirchi, A., Abedi-Koupai, J., Bavani, A.M., Madani, K., 2013. Water transfer as a solution to water shortage: a fix that can backfire. Journal of Hydrology 491, 23–39. doi:10.1016/j.jhydrol.2013.03.021.

Intergovernmental Panel On Climate Change (IPCC), 2023. Climate Change 2022 – Impacts, Adaptation and Vulnerability: Working Group II Contribution to the Sixth Assessment Report of the Intergovernmental Panel on Climate Change. 1 ed., Cambridge University Press. URL: https://www.cambridge.org/core/product/identifier/9781009325844/type/book, doi:10.1017/9781009325844.

Japan, A., 2024. River basin disaster resilience and sustainability by all. https://www.mlit.go.jp/river/shinkansen/pdf/20241120_all_en.pdf. (Accessed: Feb 16, 2025).

Kabisch, N., Frantzeskaki, N., Pauleit, S., Naumann, S., Davis, M., Artmann, M., Haase, D., Knapp, S., Korn, H., Stadler, J., Zaunberger, K., Bonn, A., 2016. Nature-based solutions to climate change mitigation and adaptation in urban areas: perspectives on indicators, knowledge gaps, barriers, and opportunities for action. Ecology and Society 21, 39. URL: http://dx.doi.org/10.5751/ES-08373-210239, doi:10.5751/ES-08373-210239.

Kochi Prefecture, Department of Agriculture, Forestry and Fisheries, Land Improvement Division, 2015. Guideline for Promoting Low-Cost Farm Road Development. Guideline. Kochi Prefectural Government. URL: https://www.pref.kochi.lg.jp/doc/2015051100249/file_contents/teikosutoshishin.pdf. accessed: 2025-06-22, PDF (in Japanese).

Kristensen, P., 2004. The DPSIR Framework. Technical Report. European Environment Agency. URL: https://www.researchgate.net/publication/253311291_The_DPSIR_Framework. presented at the workshop on a comprehensive/detailed assessment of the vulnerability of water resources to environmental change in Africa using river basin approach.

Ministry of Land, Infrastructure, Transport and Tourism, 2016. Guidelines on Urban Regeneration Plans Based on the Special Measures Law for Urban Regeneration. Technical Report. Ministry of Land, Infrastructure, Transport and Tourism (Japan). URL: https://www.mlit.go.jp/toshi/content/001609105.pdf. accessed: 2025-06-22.

Okayama Prefecture, 2019. Climate change adaptation guide for satoyama and satoumi. https://www.pref.okayama.jp/page/419837.html. Accessed: 2025-06-22.

Oki, T., Hanasaki, N., Shen, Y., Kanae, S., Masuda, K., Dirmeyer, P., 2005. 6.5 global water balance estimated by land surface models participated in the gswp2 .

Sterman, J.D., 2000. Business Dynamics: Systems Thinking and Modeling for a Complex World. Irwin/McGraw-Hill, Boston.

Su, Q., Rohila, J.S., Ranganathan, S., Karthikeyan, R., 2023. Rice yield and quality in response to daytime and nighttime temperature increase – a meta-analysis perspective. Science of The Total Environment 898, 165256. URL: https://doi.org/10.1016/j.scitotenv.2023.165256, doi:10.1016/j.scitotenv.2023.165256.

Thuiller, W., Lavorel, S., Araújo, M.B., et al., 2005. Climate change threats to plant diversity in europe. Proceedings of the National Academy of Sciences 102, 8245–8250. doi:10.1073/pnas.0409902102.

Urban, M.C., 2015. Accelerating extinction risk from climate change. Science 348, 571–573. doi:10.1126/science.aaa4984.

Yokohata, T., Tanaka, K., Nishina, K., Takahashi, K., Emori, S., Kiguchi, M., Iseri, Y., Honda, Y., Okada, M., Masaki, Y., Yamamoto, A., Shigemitsu, M., Yoshimori, M., Sueyoshi, T., Iwase, K., Hanasaki, N., Ito, A., Sakurai, G., Iizumi, T., Nishimori, M., Lim, W.H., Miyazaki, C., Okamoto, A., Kanae, S., Oki, T., 2019. Visualizing the Interconnections Among Climate Risks. Earth's Future 7, 85–100. URL: https://agupubs.onlinelibrary.wiley.com/doi/abs/10.1029/2018EF000945, doi:https://doi.org/10.1029/2018EF000945. _eprint: https://agupubs.onlinelibrary.wiley.com/doi/pdf/10.1029/2018EF000945.

Zebisch, M., Terzi, S., Pittore, M., Renner, K., Schneiderbauer, S., 2022. Climate impact chains—a conceptual modelling approach for climate risk assessment in the context of adaptation planning, in: Kondrup, C., Mercogliano, P., Bosello, F., Mysiak, J., Scoccimarro, E., Rizzo, A., Ebrey, R., Ruiter, M.d., Jeuken, A., Watkiss, P. (Eds.), Climate Adaptation Modelling, Springer International Publishing, Cham. pp. 217–224.